



Comparative Analysis and Manufacturing of Airfoil Structures Suitable for Use at Low Speeds

Satılmış Ürgün¹, Mert Gökdemir^{2*}, Sinan Fidan³

^{1,3}Faculty of Aeronautics and Astronautics, Kocaeli University, Kocaeli, Türkiye

²Institute of Natural and Applied Science, Kocaeli University, Kocaeli, Türkiye

Article History

Received: 07.02.2022

Accepted: 22.06.2022

Published: 15.12.2022

Research Article


Abstract – An aerodynamic technique to calculating lift and drag coefficients is one of the required instruments in the wing design process. During the last decades, several tools and software have been developed according to aerodynamics and numerical methods. Nowadays, aeronautical architecture requires many calculations. Today's technologists use a variety of simulation techniques to avoid a expensive model testing. This paper explains how wing profiles can be modelled using ANSYS Fluent and tested by low-speed tests considering experimental literature results. With the selected wing profile, the geometry is shaped in two dimensions and designed in three dimensions. Computational fluid dynamics (CFD) was adopted as the method for studying wing profiles. Wing profiles created at 0 to 20-degree attack angles are calculated in the simulation area equal to the actual wind tunnel scale, and equations are solved using the RNG k-Epsilon turbulence model. The process of developing the grids was realized with Ansys Mesher software. The solution stage and the result show operations were carried out with the CFD Post software. The study of the low velocity and high transport wing profiles, the drag coefficient, the lift coefficient, and the effect on the lift-drag ratio were studied using a numerical procedure. After determining the high efficiency of wing profiles, production of a selected profile began with a static examination.

Keywords – Airfoil, ANSYS, CFD, lift, NACA

1. Introduction

A wing represents a surface used to travel in an air medium perpendicular to the direction of motion to produce aerodynamic forces. A wing is a device used for producing lift with distinct contour structures. The aerodynamic efficiency of some gliders will exceed 60 or higher when expressed by the ratio of lift to drag coefficient. To achieve lift (Chitte, Jadhav, & Bansode, 2013), this means that less thrust is necessary. To obtain the limits, we require, there are two methods (lift, drag, moment coefficient, etc.). These are simulation and experiment. The item or object is inserted in the air stream for the study, and a few holes are opened on it and pressure calculation is performed. The pressure can be determined ahead of the time at each stage, and the drag rise, etc. It is used in coefficient estimation. Be it as it might, this procedure takes time, and the error margin is high. Then again, more developed PC (Personal Computer) simulations allow one to achieve the ideal characteristics in a much more limited period. The most widespread programming of PC programs is CFD (computational fluid dynamics). Inside the measurement field, the point is to illustrate. During simulation, with the assistance of the software, stream conditions are discussed in the ideal process. Simulation gives us the most rational yield characteristics. In this review, CFD programming, which provides faster performance, was preferred because the wind tunnel experiments were expensive and lengthy.

¹  urgun@kocaeli.edu.tr

²  mertgokdemir26@gmail.com

³  sfidan@kocaeli.edu.tr

*Corresponding Author

Carbon fibre reinforced polymers (CFRP) have commonly been used for about forty years in various applications. For e.g., their boss features, low weight, and high efficiency make them an enticing opportunity for certain products in different fields, including aircraft, automobile, and sea applications. In the aviation industry, the early use of composites was essentially for auxiliary non-basic applications, such as coatings and flight control surfaces (Kumara, Raghavendra, Venkata, & Ramachandra, 2012). Given the strict logistical nature of the aviation sector, various subtleties of accreditation and continuity should have appeared to precede the expanded use of these products over the airframe, recognizing that these guidelines are continuously evolving to ensure the general population's well-being (Schmid, Kruse, Korwien, & Geistbeck, 2015). The use of composites in both industrial and military airframes currently approach 40% and is used for critical load manner elements. The change was possible because of the company's dedication to this creation and the steady growth as the manufacturing approaches in the test, material, and cycle strategies. The modelling network gained the certainty of dealing with composites from such tests with numerous wins, numerous misfortunes, and exercises learned (Davies, Choqueuse, & Devaux, 2012). Despite the specialized angle, the conservative hand primarily influenced grasping composites. Compared to metal, the use of lighter-weight fabrics meant that airlines and operators could get a decent deal during operation on fuel prices. It was found that with every pound saved of weight; a saving of \$46 can be made, accepting \$3.44 per gallon of jet fuel (Aviation Outlook, 2021).

With respect to composites, the basic cost factors are the crude material, tooling, function, amount of manufacturing, the scale of output, and machinery. In such areas, any changes will theoretically bring down the prices. With the developments in these fields over the next few decades, the cost of constructing plastic products is agreed to be extreme for metallic materials, which would make them a substantially greater candidate for potential items (Shama, Simha, Rao, & Kumar, 2020). By combining two separate materials that have properties that are obtained by consolidating multiple elements, composite materials are produced. Composite materials are often referred to as composition materials, which are the materials created using at least two constituent materials with various physical and synthetic properties, which coat a substance with different characteristics from its constituents when consolidated. In addition, the constituent components for composites are referred to as 'Reinforcement material and matrix material' that are correctly mixed to achieve the optimal properties, such as dimensional protection, electrical opposition, etc. To obtain adequate consistency in the composite material, the re-enforcement material, and the matrix material must be joined in suitable places. In general, the efficiency of the composite materials depends on the ratio of the reinforcement material and the matrix material. There is a big overview of composite materials, including polymer matrix, ceramic matrix, and metal matrix composites, which are commonly used in the industry. Current research and engineering involve a completely different category of cutting-edge materials, particularly in the areas related to shipping, aviation, and military architecture (Choubey et al., 2018, Lee et al., 2017, Delogu et al., 2017, Karthigeyan et al., 2017, Yadav et al., 2017). For aircraft frames, exceptional corrosion, and fatigue-damage tolerance, composites have demonstrated weight savings. Applications for commercial aircraft have gone from limited flight control surfaces to an ever-increasing number of critical structures (Schwartz, 1992).

Onour (2011) conducted the hypothetical study of AG24, AG35, AG455ct, CAL1215j, CAL2263m, and CAL40411 profiles. Using MATLAB tools at low Reynold's coefficients, test estimations were obtained. As per the results, in the low Reynolds number, the maximum value for the angle of attack and drag coefficient was achieved, and in the high Reynolds number, the minimum value was reached. A high Reynolds number and a minimum value for a low Reynolds number were obtained for the highest lift coefficient/angle of attack. The comparative results show the AG35 airfoil is the most acceptable profile for the design.

Parashar (2015) planned the study of NACA2415, NACA23012, and NACA23105 airfoils, using the GAMBIT and Fluent commercial CFD systems. For flow, using the regular $k-\epsilon$ disruption model, momentum continuity equations are studied. With CATIA's guidance, 2D wing geometries were obtained at a chord ratio of 0.5 C. At differing attack angles at -15 and +15 degrees, the two streamlined limits were calculated. In determining aerodynamic efficiency, these two limits are of prime importance. Contrary to NACA2415, NACA23015 and NACA23012, at the extreme angle of attack, NACA23012 airfoil produced the least drag at = 0. If the limit is NACA23012 (at the lift coefficient), the lowest drag has been reached.

In this study, Syamsuar, et al., (2016) proficient low-speed airfoil determination and optimization was conducted using multi-directional analysis for unmanned aerial vehicles. The enhancement period involves low-speed airfoil details and design optimization measures as shown by the design needs provided. In unmanned

aerial vehicles, the stability criteria are of high importance due to low clutter and poor stability. Using computational fluid dynamics (CFD), tests were conducted. In XFOIL and ANSYS, studies were conducted using the model of Navier strokes. In selecting the required airfoil for the design criteria, the weighting technique was used to find the greatest weight value. When the calculations of lift, drag, moment coefficient, and angle of attack were compared with 29 wing profiles as a database, the TL54 wing profile got the highest score.

In the Jony (2014), The drag lift force and overall pressure distributions affecting the NACA6409 and NACA4412 profile profiles were also considered, and flow analysis was analysed. Different variables were obtained by adjusting the angle of attack. In the analysis, the ANSYS Workbench 14.5 programming finite element approach and computational fluid dynamics (CFD) were used to render connections. On the top surface of the NACA4412 airfoil; there is less negative pressure than on the top surface of the NACA6409 airfoil. Separately, the lift/drag ratios for NACA4412 are 3.365 and 5.382 for 0 and 5 degrees. Then again, for the NACA6409 profile, the lift/drag proportions are 0.39 and 0.66 at the attack angle between 0 and 5 degrees, individually. The optimal profile should regularly have a high proportion of lift/drag. The NACA4412 profile is more suitable for aerodynamic applications by comparing the results.

Based on the examples above, the wing profiles, which are widely used today, were analysed at varying angles of attack, and the targeted optimum profile was tried to be obtained. Fuel consumption is of high importance for operator companies and developers in today's aircraft. The way to increase fuel consumption on an aircraft or airfoil is to have the best efficiency that can be requested from its profile. Considering these interests, our aim in our study is to compare 4 different wing profiles in terms of their specific characteristics (carrying, drag coefficient, aerodynamic efficiency) and to produce the most efficient profile in order to set an example for later studies. Creation from composite material was chosen as a new technique in the production of the wing profile, which was examined using simulation software. It has been determined that the application potential of composite material wings and load-bearing parts in wing structures of the proposed size is high. Because of their complex geometry, load-bearing parts inside the wing are challenging to produce from composite material. Precision molding and surface smoothing procedures were used to ensure that the tolerances and dimensions of the composite load-bearing parts were met throughout the manufacturing phase. During assembly, a holistic structure was built by using unique processes to each piece manufactured as a composite part in order to construct a full wing structure.

2. Design and Analysis

The main feature in determining the consistency of acceptance is finite element mesh since the nodes generated characterized the performance parameters for the analysis (Kanesan, Mansor, & Abdul-Latif, 2014). The primary motive behind any configuration of the airfoil is to create an airfoil that offers a more notable lift calculation without drag expansion. Even, without stalling, the airfoil should have the option of operating at high angles of attack (Fertis, 1994). The philosophies of airfoil and wing design have taken huge strides forward with the accessibility of fast computing resources that consider precise aerodynamic efficiency targets. These aims are mainly to improve an efficiency measurement, such as the proportion of lift over drag, or its item with flight Mach number in higher-speed systems. The need for extended lift at higher flight levels, with drag held low has prompted the creation of information bases for streamlined design (Sobieczky, 1999). Currently, wing prototypes are not made by hand, but with the aid of PCs. Two classes of methods are usually based on these new computerized modelling techniques. They either use quasi-experimental equations or use lower-fidelity mathematical devices to help determine the appropriate limits, such as streamlined properties, flight efficiency, applied loads (Jaroslaw, & Raphael, 1996, Cm Erep, 1986). There are several steps toward developing a wing and carrying it to the testing level. The importance of the demand opportunity and the needs of analysis and the area of use (Anderson, 1999, Anderson, 2001) form it. It is important that before the design can begin, the task needs to be characterized. The corresponding stage is to create a concrete design following the design proposal. For another aircraft, the conceptual architecture constructs the main general scale and structure. It requires the load evaluations and the determination of simplified qualities that would be most relevant to the prerequisites of the mission expressed in the proposal for a design. The iterative circle in the flow map demonstrates this. The design transitions to the following level, which is the preliminary design (Meganathan, 2014), at the point where the mission prerequisites are met. It is important to distinguish and address conflicts of need and to place the required measure of focus on specifications that arise as the concept matures. The visible proof and regulation of significant performance attributes (Henne, 1990), are the key

challenge in airfoil configuration. During the wing design process, 18 boundaries must be resolved. They are as per the following:

1. Wing reference (or planform) area (S_w , S_{ref} or S).
2. Number of wings.
3. Vertical position relative to the fuselage (high, mid-, or low wing).
4. Horizontal position relative to the fuselage.
5. Cross-section (or airfoil).
6. Aspect ratio (AR).
7. Taper ratio (λ).
8. Tip chord (C_t).
9. Root chord (C_r).
10. Mean aerodynamic chord (MAC or C).
11. Span (b).
12. Twist angle (or washout) (α_t).
13. Sweep angle (Λ).
14. Dihedral angle (Γ).
15. Incidence (i_w) (or setting angle, α_{set}).
16. High-lifting devices such as flap.
17. Aileron.
18. Other wing accessories.

Of the above considerable rundown, until this point (during the preliminary design step), only the first (i.e., planform region) has been determined. An iterative period is the wing configuration, and the determinations/computations are normally repeated a few times (Sadraey, 2013). In a wing structure, where the airflow first meets, the leading edge is known, and the trailing edge is known when the airflow leaves. The wing cross-section beamline (veter) is called the line joining these two points. The arc that goes around the middle of the upper and lower surfaces and joins the leading edge and the chord is known as the trailing edge. If analysing, there are two variables that we consider thickness and chord. The highest curvature of the NACA23012 airfoil is 2% of the beam length and 12% of the beam length is the maximum thickness. In low-speed airplane wings, the wing area of NACA23012 is commonly used. The proportion of thickness in the NACA4412 profile is 12% and the proportion of curvature is 4%. Airfoil NACA4412 has a large range of aircraft applications, from wind turbines to air cushion aircraft. The TL54 is usually favoured because, like Rc Motors, it creates lower profile drag at low speeds. The proportion of thickness in the TL54 profile is 9.99% and the proportion of curvature is 2.41% like hovering boats, miniature quad copters etc. The AG35 profile used in low speed unmanned aerial vehicles has an 8.7% thickness and a 2.3% curvature proportion. It was only developed when the aerodynamic efficiency 4412 wing profile achieved the highest score. The design process must be undergone before a component can be made. Two major steps are performed in this step, to be specific to the drawing and examination of the component. A specification is rendered during the section's drawing time in conjunction with the role where it will be used. In this design, things are mulled over, for example, function and aesthetics. Nonetheless, it is not clear if the operational conditions of the design carried out would accomplish the purpose here. Significant engineering measurements and observations should be made to address this question.

Aerodynamic coefficients depend on attack angle, geometry (geometry of the profile, geometry of the wing, configuration of the airplane), number of Reynolds, and number of Mach. The airfoil lift and drag coefficients are experimentally acquired or applications that can be used during profile selection causes estimated values to be used. A PC with a 3.5 GHz 4-core AMD Ryzen 5 1500X CPU, 16 GB RAM, and a 64-bit Windows 10 operating system was used for the simulation. To evaluate the fluid streaming over the profiles, the program ANSYS Fluent (version-16) was used. To maximize outcomes, an organized mesh is used. The angle of attack is defined as the angle on the plane or wing between the air and relative wind over the wing and a reference line (veter). This angle determines the aerodynamic powers of drag that exist.

Table 1
Specification of input parameters

Parameters	Magnitude
Solver Type	Pressure-based
Time	Steady
Velocity of flow	22.22 m/s
Operating temperature	300 K
Operating pressure	1 atm
Viscous model	K-epsilon (2 eqn)
Density of fluid	1.225 kg/m ³
AoA of airfoil	Steady
Kinematic viscosity	1.79E-05
Reynolds number	Vary with air velocity
Number of iterations	1000
Angle of attack	0 to 20
Solution method	Second order upwind
Length	1 m

The k-ε realizable turbulence model was used to assess the aerodynamic efficiency of the two-dimensional flow on the wing profiles in computational fluid dynamics. The input values are specified in Table 1 above.

2.1. Realizable k-e turbulence Model

The most well-known model used in Computational Fluid Dynamics (CFD) to simulate average flow properties under turbulent flow conditions is the K-epsilon turbulence model. To view turbulence flow, it has two additional transport equations. These two models of equations, for instance, convection and diffusion, help to understand the impacts of turbulent energy.

- The first variable is turbulent kinetic energy, k
- The second variable is the turbulent distribution, ε

The variable determines the turbulence scale, while the primary variable k determines the energy in turbulence (Jones, & Launder, 1972, Launder, & Sharma, 1974). The K-epsilon model can be derived as follows:

$$\frac{\partial}{\partial t}(\rho k) + \frac{\partial}{\partial x_j}(\rho k u_j) = \frac{\partial}{\partial x_j} \left[\left(\mu + \frac{\mu_t}{\sigma_k} \right) \frac{\partial k}{\partial x_j} \right] + P_k + P_b - \rho \epsilon - Y_M + S_k, \frac{\partial}{\partial t}(\rho \epsilon) + \frac{\partial}{\partial x_j}(\rho \epsilon u_j) = \frac{\partial}{\partial x_j} \left[\left(\mu + \frac{\mu_t}{\sigma_\epsilon} \right) \frac{\partial \epsilon}{\partial x_j} \right] + \rho C_1 S \epsilon - \rho C_2 \frac{\epsilon^2}{k + \sqrt{\nu \epsilon}} + C_{1\epsilon} \frac{\epsilon}{k} C_{3\epsilon} P_b + S_\epsilon \tag{2.1}$$

Turbulent viscosity is modeled as follows,

$$\mu_t = \frac{\rho C_\mu k^2}{\epsilon} \tag{2.2}$$

K generation can be written as,

$$P_k = \overline{\rho u_i u_j} \frac{\partial u_j}{\partial x_i} \tag{2.3}$$

S is the modulus of the average strain rate tensor defined as:

$$S \equiv \sqrt{2 S_{ij} S_{ij}} \tag{2.4}$$

The model constants used for these equations are:

$$C_{1\epsilon} = 1.44, C_{2\epsilon} = 1.92, C_{3\epsilon} = -0.33, C_{\mu} = 0.09, \sigma_k = 1.0, \sigma_{\epsilon} = 1.3 \tag{2.5}$$

2.2. Lift to-drag ratio

The lift-to-drag ratio, or L/D ratio, in aerodynamics is the division of the lift produced by a wing or vehicle by the aerodynamic drag it creates by flying. One of the key targets of wing/airplane architecture is a higher or greater L/D proportion. Low drag offers fuel savings and improved climbing performance, as the required lift is acclimatized to the weight. Lift/drag is the speed vector that shows in the 2D map. The image produces a U shape in almost all situations since the drag has two main components. Wind tunnel flight simulation, measurements, or testing (Wu, Sun, Luo, Sun, Chen, & Sun, 2018), can calculate lift-to-drag ratios. The obtained aerodynamic efficiency values are shown in Table 2.

Table 2
Aerodynamic efficiency comparison

AoA	4412	AG35	23012	TL54
0	16.94	19.3	7.28	8.33
5	12.54	13.85	15.52	13.78
10	8.78	8.87	10.27	9.1
15	6.5	6.19	7.25	5.91
20	5.09	3.45	5.47	2.82

2.3. Drag and Lift Coefficient

The drag coefficient in fluid dynamics is a dimensionless quantity in a fluid medium, such as air or water that is used to measure an item's drag or opposition. A low drag coefficient allows an object to have less aerodynamic drag. The drag coefficient is continuously bound to a particular region of the surface (Stollery, 2017). In the drag coefficient condition, the drag coefficient utilizes the wing region as the reference region. The drag coefficient is an unfathomable value that is used to determine the fluid opposition of moving objects. The lift force (coefficient) is a mechanical aerodynamic force generated by the fluid flowing through a rigid body, and this force opposes and maintains the weight of the moving mass in the air. A vector acts against the flying item's centre of pressure. The lift is obtained from the fluid velocity differential around the flying object. If the object is flowing through or fluid, streaming through an object does not make a difference. Usually, the lift coefficient is determined without dimensions (Sharma, 2016).

$$c_D = \left(\frac{2F_D}{\rho u^2 A} \right), c_L = \left(\frac{2F_L}{\rho u^2 A} \right) \tag{2.6}$$

Table 3
Lift coefficients

AoA	4412	AG35	23012	TL54
0	0.192	0.1467	0.043	0.08
5	0.439	0.3866	0.2795	0.3142
10	0.685	0.6342	0.527	0.5411
15	0.936	0.8713	0.775	0.722
20	1.171	0.7433	1	0.7615

Table 4
Drag coefficients

AoA	4412	AG35	23012	TL54
0	0.011	0.0076	0.0059	0.0096
5	0.035	0.0279	0.018	0.0228
10	0.078	0.0715	0.0513	0.0594
15	0.144	0.1407	0.1068	0.122
20	0.23	0.2151	0.1827	0.27

The above Table 3 and 4 shows the lift and drag coefficients. The data obtained are calculated depending on the lift coefficient (c_L), drag coefficient (c_D), free flow velocity (u), free flow density (ρ) and profile veter length. For the NACA23012 and NACA4412 profile, the lift coefficient reached the threshold of 1 value.

3. Manufacturing

After the review and saved in phase format our NACA4412 airfoil was modelled in the SolidWorks software. Then, by running an output in ANSYS Mechanical, the material properties of the profile (ribs and stringers) to be used are allocated. The manufacturing process eventually began. In our research, we chose EPIKOTETM Resin MGS ® L285 (Epoksi hexion, 2021), which are used with extremely strong mechanical and thermal properties in aviation and model aircraft. For the mold, polystyrene material (white foam) was used. The use of polystyrene is effective, so it will be useful for airfoil model growth. Only the NACA4412 airfoil with a 2750 mm chord and a 2300 mm span width was planned. There are nine ribs and five stringers of skin in the wing system. As seen in Figure 2, the wing structure is shaped.

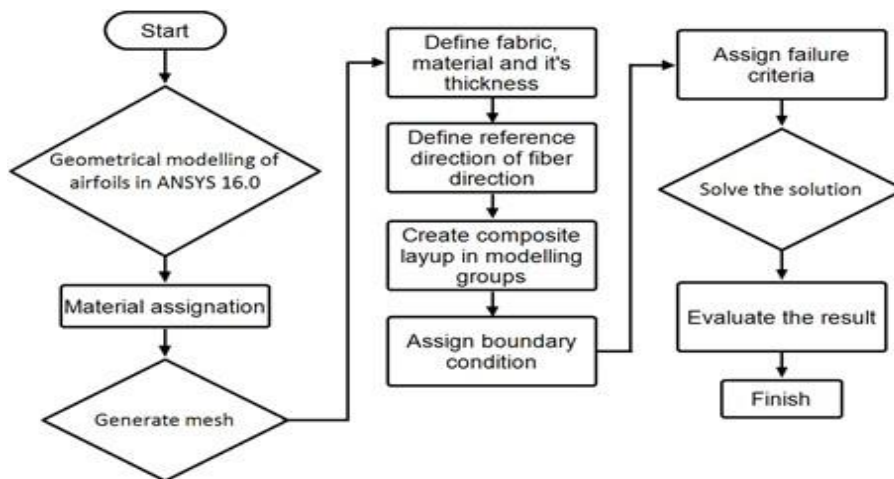


Figure 1. Design parameters

In Figure 2 above, the steps to be taken to build a wing profile are given. First, the wing profile was modelled with Ansys package program. After the material assignment, the meshing process is performed to determine the thickness and fabric of the material. After modelling, fault assignment is made and the results are evaluated, and the design is completed. The method proceeds in the event of a potential mistake by returning to the previous stage. Airfoil structure and construction phase are given in figure 3 and 4.



Figure 2. Wing structure

Two carrier aluminum spars were used in the production of the blade shown in Figure 3. Ribs are primarily produced with XPS polyurethane and covered in 3 layers with epoxy and glass fiber fabric. Ribs are connected at different points with stringers produced with glass fiber fabric and epoxy. Finally, as can be seen in Figure 4, the wing skeleton formed is covered with glass fiber fabric and epoxy, thus creating a very light and strong wing.



Figure 3. Construction of NACA4412 profile

4. Results and Discussion

Using a denser mesh of the wing area, 727946 Elements and 167323 Nodes were made for a performance that is more accurate. As the leading and trailing edges are the focuses that first take the air and leave the air, in these regions the solved equations should be more sensible. These regions are, however, filled with a mesh of 0.002 units. To define the boundary region of the flow, an extra zone has been inserted along with the wing profile. The air's inlet and exit points are overcome. The chord was picked to be 1 meter and the flow area behind the wing was 10 meters of laminar flow. The goal of this analysis is to use the ANSYS Fluent software

to generate a virtual model of the external flow across the wing profiles AG35, NACA4412, NACA23012, and TL54 and to validate it by measuring it at a low speed (22.22 m/s) in the light of the experimental data acquired from the literature. Changing the airfoil's attack angle indicates important speed changes. There is a greater value for the velocity on the top surface of the wing than on the lower surface. As a result, the friction on the upper surface is minimal relative to the wing's lower surface. The entity would shift from the higher-pressure zone to the lower pressure region, as per Bernoulli's theorem. Therefore, on the wing, lift exists. The turbulence grows, as in the writing, as the angle of attack increases at the end of the study. The velocity or AOA must be altered to keep up the laminar flow. The wing angle and velocity of the incoming fluid (air) were held steady throughout the simulation. As a working setting, 15°C 1 ATM pressure and 22.22 m/s speed were used. The methodology of the Coupled Scheme approach was used, which is time-dependent and can arrive at a fast solution. Since our geometries are large, long and there are various regions with pressure variations over them, the Realizable model was picked.

In the rest of the study, the pressure, and velocity-dependent behaviours of all airfoils at 0 and 20 degrees were envisioned. The high-pressure zone at the leading edge and the low-pressure zone on the lower surface of the airfoil system can be seen from the contours. The photos in the figures demonstrate simulation effects of static pressure and velocity changes with the K-epsilon turbulence model at an angle of attack of 0° to 20°. The profile of NACA4412 reached 28.8 m/s on the upper surface of the wing at the maximum velocity. At the same time, as the velocity-pressure is equal to the opposite, the NACA4412 profile with ~ (-250) Pa. was the least pressure on the wing. This makes us the most notable lift at 0° on the NACA4412 profile. While the profiles tend to display smooth flow, the maximum speed of the NACA4412 profile was 48.4 m/s and the maximum speed of the NACA23012 profile was 48.2 m/s. At the leading edges, the NACA4412 and NACA23012 profiles are somewhat stalled, and the entire profile has dropped into stall by decreasing the speed at the trailing edges to 0 m/s. The analysis provides improved results in all profiles below 16 degrees of attack angle for 22.22 m/s velocity. The results show that the predicted drag coefficient in the K-epsilon turbulence model is in good accordance with the experimental evidence. The findings obtained from the simulations demonstrate that lift and drag coefficients for the wings are not greatly influenced by the free flow velocity. Compared to low speeds, the airfoil experiences an increase in lift coefficient and a decrease in drag coefficient at high altitudes. The disparity between airfoil lift and drag coefficients can be explained by the existence of low-velocity separation at a lower attack angle as opposed to high velocity. In different scenarios during the cycle, the simulation provided incredibly interesting results for pressure distribution. Compared to the root, the lower static pressure distribution near the wing tip affirms the three-dimensional movement across the wing. As the angle of attack increased, it was observed, and values increased. The stall happened after 15 degrees because the speed diminished to 0 m/s. With the flow rate, the pressure on the lower and upper surfaces of the profile grew. This result revealed that when in the air, a wing profile or airplane needed to exceed a certain speed to take off and fall below a specific speed. The literature has stated that the pressure differential increases with the effect of the lift on the wing, the difference of pressure below or more with the speed and angle of attack on the wing. The analysis of four airfoils indicates that in applications where the theory is attempted, the NACA4412 airfoil configuration should be preferred as it achieves greater lift force with the least drag force.

4.1. Structural Static Analysis of NACA4412 Airfoil in Ansys

An airfoil was previously developed and stored in the Solid Works program. In Ansys Workbench, stage format is entered. In the engineering details in the Ansys library, the content properties are entered. In Figure 5 below, the material properties are added. The body (fixed support) has one end of the wing fixed to it. The wing's other end is open. In this manner, deformation and stress values added to the wing can be obtained by correcting one foot. Analysis of stress is essential to structural architecture. Wing construction geometry, with the most optimal range of structural parameters such as material and width, should be light and robust to critical loads.

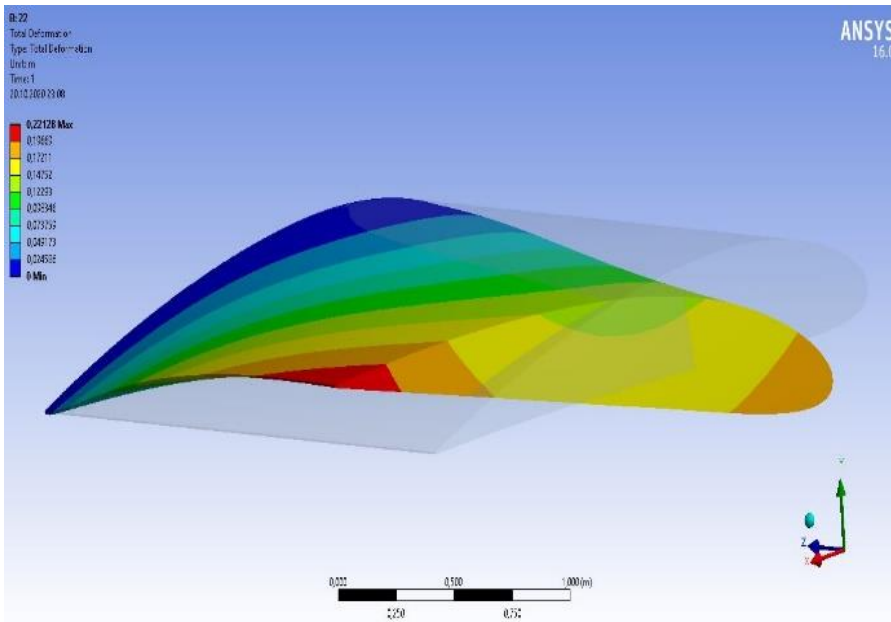


Figure 4. Total deformation on NACA4412

The cumulative displacement of the wing at the pressure and speeds applied to the NACA4412 airfoil is 0.221 m, as can be seen in the visuals above. These values give us knowledge about the changes in the angle of the base and the wings' deformation.

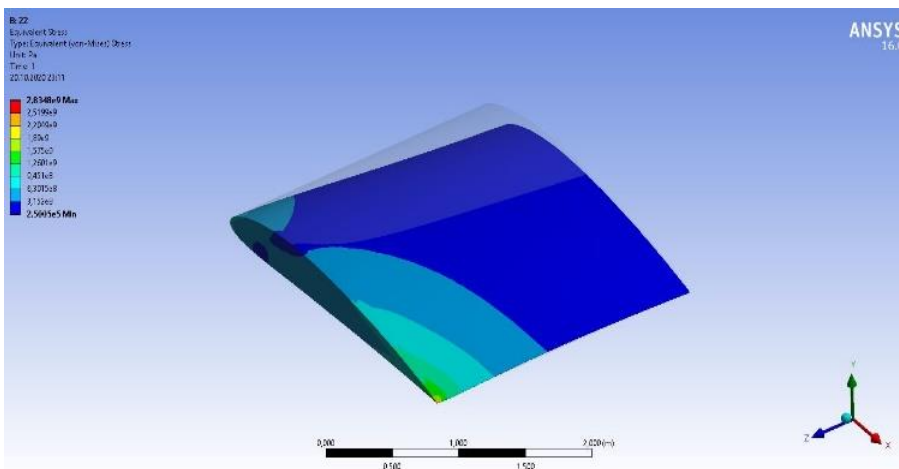


Figure 5. Von-mises stress

In Figure 6 above, Von-mises stress is observed. The stress distribution on the airfoil decreases from the wing root to the wing tip. The stress on the wing is observed from the root of the wing. It is colored lighter at the root of the wing and with a darker color chart as it moves away from the root of the wing.

4.2. Modal Analysis of NACA4412

To perform modal analysis to determine the wing model's normal frequency and mode shape. The wing subjected to unpredictable aerodynamic loads will easily fail due to resonance if the normal frequency of the wing coincides with the frequency of the load. For detailed dynamic analysis of wing models in the future, modal analysis is a prerequisite. A classic problem of self-value is modal analysis. The kinematic equation is the basic harmonic vibration of the free vibration of the structure, which means that the displacement meets the function of the sinus.

$$x = x \sin(\omega t) \tag{4.1}$$

$$([K] - \omega^2[M])\{x\} = \{0\} \tag{4.2}$$

Equation (8) is a classic eigenvalue problem, the equation eigenvalue is, the extraction of a root is auto oscillation circular frequency, and the natural vibration frequency is. Vector related to is mode of vibration related to natural vibration frequency (Yongchang, Zhang, Li, Wang, & Tang, 2017).

Table 5
Mode Frequencies

Mode	Frequency [Hz]
1,2	0
3	2.8184e-005
4	6.6268e-005
5	1.4164e-004
6	2.8383e-004

The consequence of the modal analysis is that, under these frequencies, the frequencies of 6 distinct modes and the deformation values are obtained. In the typical free frequency, the profile does not vibrate, but due to self-weight, certain timeline vibrations occur. Each natural frequency has a distinctive mode shape comparable to different amplitudes. Different modes can be seen in the Figure 7 below (deformed and unreformed).

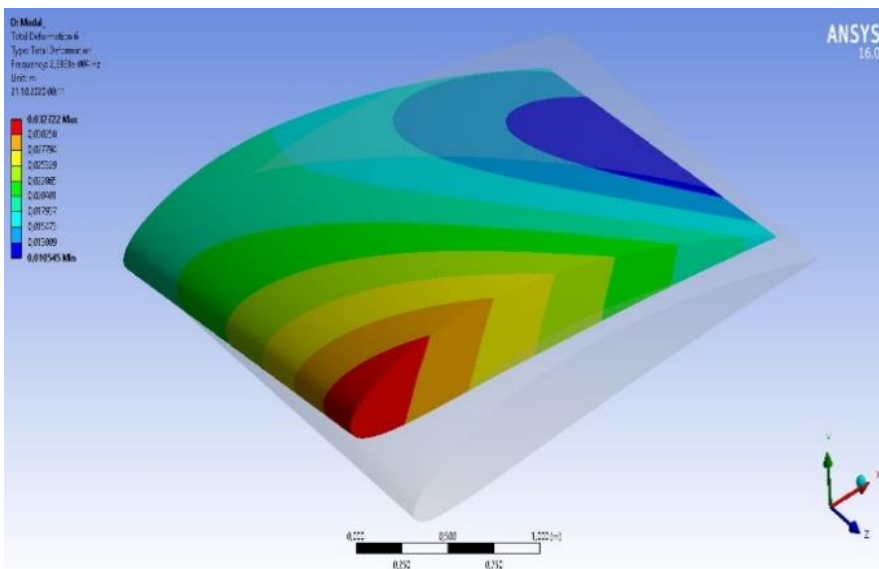


Figure 6. Modal analysis

The most appealing thing is to select an adequate airfoil profile in an airplane configuration. In this way, under the boundary conditions indicated for that airplane, the ideal measure of lift can be made. The most important values to be considered for the best possible aerodynamic configuration of the wing are lift-drag ratio, lift and drag coefficient. CFD simulation was used in this analysis to analyse the flow area and aerodynamic properties of airfoils AG35, NACA4412, NACA23012, and TL54, and numerical simulation was conducted at different attack angles (0°, 5°, 10°, 15°, and 20°). Using a realizable k-epsilon turbulence model and finite volume diagrams, flow properties were roughly analysed. It has been shown that the drag coefficient also increases as AoA increases. This rise is due to the increasing separation zone on the airfoil's upper surface and the increased pressure drag becoming greater than that under the airfoil. The lift generated by the wing profile increases as the angle of attack increases. The lift force decreased after the stall angle (15°). The discrepancy in the flow characteristics of the wing profiles can be deduced as follows, according to this study:

Max:

- 0°-5° AoA, AG35,
- 5°-15°-20° AoA, in the NACA23012 profile

Max:

- 0°-5°-15°-20° AoA, in the NACA4412 profile

Max:

- 0°-5°-10°-15° AoA, NACA4412
- 15°-20° AoA, in the TL54 profile

Even though the NACA4412 profile has the second-best performance among the profiles in terms of aerodynamic efficiency at reference values, the maximum drag and lift coefficient at all attack angles (0°, 5°, 10°, 15°, 20°) has been identified. Accordingly, considering these values under different circumstances, the NACA4412 airfoil should be selected for the specified conditions from among these four airfoils. In the 'static structure' portion of the Ansys workbench, pick the content first. A network of solutions, called meshes, was generated on the wings after choosing the materials. In addition, the values of deformation and Von-Mises stress were obtained. The contrary was not found, given the characteristics of the products we picked depending on the findings of the study. The consequence of the equation is that the final load does not surpass the safe value. The maximum value of the corresponding stress is 2.8348e9 Pa., with a gross wing displacement of 0.221 m at the pressure and speeds applied to the NACA4412 airfoil. These values give us knowledge about the changes in the angle of the base and the wings' deformation.

5. Conclusion

A plane wing construction is developed and constructed in this examination using Solid Works, a 3D modelling tool. The Rib and Spars provided structure for the wing. Typically, aluminium composites are components that are used for aircraft wings. Anyway, we used polystyrene for ribs, the spars, the skeleton, and the fibreglass composite for exterior coating in our own review. In the Ansys programme, a structural static analysis was carried out, which prevented the cost of experience. The deflection and strain on the wing were acquired through static analysis. The module was analysed to determine the normal wing frequency, which was subjected to continuous vibration during the flight. There is a possibility that the composite structure will resonate and fail to accomplish its mission. Today, the use of air vehicles for recreational, military and commercial purposes is becoming more frequent. Manufacturers require the design of the blades to satisfy the desired criteria. This includes developing blade geometries in response to needs, modifications, etc. Our study aims to lead the way for future studies by comparing wing profiles, which have different uses in aviation, with each other. Consequently, among the AG35, NACA 4412, NACA 23012, and TL54 airfoils that are commonly used in various aviation applications, the NACA 4412 airfoil with the best efficiency should be preferred. Since the study's conclusions were not validated in actual tests, outcomes will vary among designs. Afterwards, inside a larger flow volume and a more continuous arrangement organization, flow analysis may be presented within the work of this approach. Attacks, hyper-extends, and heated responses should be noted for further investigation. Landing gear, engine, and other analyses should be verified later in the construction stage.

Author Contributions

Satılmış Ürgün: Conceived and designed the analysis.

Sinan Fidan: Collected data and performed the analysis.

Mert Gökdemir: Performed statistical analysis and wrote the paper.

Conflicts of Interest

The authors declare no conflict of interest.

References

- Anderson, J. D. (1999). Aircraft Performance and Design, Boston, WCB/McGraw-Hill. Retrieved from: https://www.academia.edu/40606141/AIRCRAFT_PERFORMANCE_AND_DESIGN
- Anderson, J. D. (2001). Introduction to Flight, McGraw-Hill, New York. Retrieved from:

- <http://ae.sharif.edu/~iae/Download/Introduction%20to%20flight.pdf>
- Aviation Outlook. (2021). Retrieved from: <https://www.compositesworld.com/articles/aviation-outlook-fuel-pricing-ignites-demand-for-composites-in-commercial-transports>.
- Chitte, P., Jadhav, P. K., & Bansode, S. S. (2013). Statistic and Dynamic Analysis of Typical Wing Structure of Aircraft Using Nastran. *International Journal of Application or Innovation in Engineering & Management*, ISSN: 2319-4847.
- Choubey, G., Suneetha, L., Pandey, K. M. (2018). Composite Materials Used in Scramjet- A Review. *Materials Today: Proceedings*, 5, pp. 1321-1326. doi: <https://doi.org/10.1016/j.matpr.2017.11.217>
- Davies, P., Choqueuse, D., & Devaux, H. (2012). Failure of Polymer Matrix Composites in Marine and Off-shore Applications. *Failure Mechanisms in Polymer Matrix Composites*. 1st ed., Woodhead Publishing, Cambridge, pp. 300-336. ISBN-13: 978-1845697501.
- Delogu, M., Zanchi, L., Dattilo, C.A., Pierini, M. (2017). Innovative Composites and Hybrid Materials for Electric Vehicles Lightweight Design in a Sustainability Perspective. *Materials Today Communications*, 13, pp. 192-209. doi: <https://doi.org/10.1016/j.mtcomm.2017.09.012>
- Epoksi hexion. (2021). Retrieved from: <https://www.dostkimya.com/tr/urunler/epoksi-sistemler/laminasyon-epoksi-hexion-mgs-l285-sistemi>
- Fertis, D. G. (1994). New Airfoil-Design Concept with Improved Aerodynamic Characteristics. *Journal of Aerospace Engineering*, 7(3), pp. 328-339. doi: [https://doi.org/10.1061/\(ASCE\)0893-1321\(1994\)7:3\(328\)](https://doi.org/10.1061/(ASCE)0893-1321(1994)7:3(328))
- Henne, P. A. (1990). *Applied Computational Aerodynamics*, Washington DC, American Institute of Aeronautics and Astronautics. ISBN: 093040369X 9780930403690
- Jaroslaw, S., Raphael, T. (1996). Multidisciplinary Aerospace Design Optimization: Survey of Recent Developments, *Structural Optimization*, 14, pp. 1-23. doi:10.1007/BF01197554
- Jones, W. P., Launder, B. E. (1972). The Prediction of Laminarization with a Two-Equation Model of Turbulence. *International Journal of Heat and Mass Transfer*, vol. 15, pp. 301-314. doi: [https://doi.org/10.1016/0017-9310\(72\)90076-2](https://doi.org/10.1016/0017-9310(72)90076-2)
- Jony, H. N., Hossain, S., Raiyan, F. M., Akanda, U. N. M. (2014). A Comparative Flow Analysis of Naca6409 and Naca4412 Aerofoil. *International Journal of Research in Engineering and Technology*, 03(10), pp. 342–350.
- Kanesan, G., Mansor, S., Abdul-Latif, A. (2014). Validation of UAV Wing Structural Model for Finite Element Analysis. *J Teknol*, 71, pp. 1-5. doi:10.11113/jt.v71.3710
- Karthigeyan, P., Raja, M. S., Hariharan, R., Karthikeyan, R., Prakash, S. (2017). Performance Evaluation of Composite Material for Aircraft Industries. *Materials Today: Proceedings*, 4, pp.3263-3269. doi: <https://doi.org/10.1016/j.matpr.2017.02.212>
- Kumara, S. M., Raghavendra, K., Venkataswamy, A. M., Ramachandra, H. V. (2012). Fractographic Analysis of Tensile Failures of Aerospace Grade Composites. *Material Research*, 15(6), 990-997. doi: <https://doi.org/10.1590/S1516-14392012005000141>
- Launder, B. E., Sharma, B. I. (1974). Application of the Energy Dissipation Model of Turbulence to the Calculation of Flow Near a Spinning Disc. *Letters in Heat and Mass Transfer*, vol. 1, no. 2, pp. 131-138. doi: [https://doi.org/10.1016/0094-4548\(74\)90150-7](https://doi.org/10.1016/0094-4548(74)90150-7)
- Lee, J. Y., Yan, J. A., Chua, C. K. (2017), Fundamentals, and applications of 3D printing for novel materials. *Applied Materials Today*, 7, pp. 120-133. doi: <https://doi.org/10.1016/j.apmt.2017.02.004>
- Meganathan, V. (2014). Aircraft Design Project-I: Heavy Business Jet. Retrieved from: https://www.researchgate.net/publication/263850415_AIRCRAFT_DESIGN_PROJECT_I_Heavy_Business_Jet
- Onour, H. K., Jahangiri, M., Sedaghat, A. (2011). Theoretical Aerodynamic Analysis of Six Airfoils for Use on Small Wind Turbines, *Proceedings of the 1st International Conference on Emerging Trends in Energy Conservation – ETEC*, Tehran, Iran, 20-21 November.
- Parashar, H. (2015). Calculation of Aerodynamic Characteristics of NACA 2415, 23012, 23015 Airfoils Using Computational Fluid Dynamics (CFD). *International Journal of Science, Engineering and Technology Research*, 4(3), pp. 610–614. Retrieved from: <http://ijsetr.org/wpcontent/uploads/2015/03/IJSETR-VOL-4- ISSUE-3-610-614.pdf>
- Sadraey, M. (2013). *Aircraft Design: A Systems Engineering Approach*, 1st ed., Wiley, New Hampshire. ISBN: 978-1-119-95340-1.
- Schmid Fuertes, T.A., Kruse, T., Korwien, T., & Geistbeck, M. (2015). Bonding of CFRP Primary Aerospace

- Structures - Discussion of the Certification Boundary Conditions and Related Technology Fields Addressing the Needs for Development. *Composite Interfaces*, 22(8), pp. 795-808. doi: <https://doi.org/10.1080/09276440.2015.1077048>
- Schwartz, M. (1992). *Composite Materials Handbook*, 2nd ed., McGraw-Hill, New York. ISBN: 0070558191 9780070558199
- Shama, R. N., Simha, T. G. A., Rao K, P., Kumar, R. G. V. V. (2020), Carbon Composites Are Becoming Competitive and Cost Effective, Infosys Limited, Retrieved from: <https://www.infosys.com/engineering-services/white-papers/Documents/carbon-composites-cost-effective.pdf>
- Sharma, S. (2016). An Aerodynamic Comparative Analysis of Airfoils for Low-Speed Aircrafts, *International Journal of Engineering Research*, V5 (11), pp. 525–529. doi:10.17577/IJERTV5IS110361
- Sobieczky, H. (1999). Parametric Airfoils and Wings, In: Fujii K., Dulikravich G.S., Recent Development of Aerodynamic Design Methodologies, Notes on Numerical Fluid Mechanics (NNFM), vol 65, Vieweg+Teubner Verlag, doi:10.1007/978-3-322-89952-1_4
- Stollery, J. L. (2017). Aerodynamics, Aeronautics and Flight Mechanics, *In Proceedings of the Institution of Mechanical Engineers, Part G: Journal of Aerospace Engineering*, Vol. 211, doi: <https://doi.org/10.1177/095441009721100102>
- Syamsuar, S., Djatmiko, E. B., Erwandi, E., Mujahid, A. S., Subchan, S. (2016). The Hydroplaning Simulation of Flying Boat Remote Control Model, *Jurnal Teknologi*, 78(6), pp. 191–197, doi: <https://doi.org/10.11113/jt.v78.4267>
- Wu, W., Sun, Q., Luo, S., Sun, M., Chen, Z., & Sun, H. (2018). Accurate calculation of aerodynamic coefficients of parafoil airdrop system based on computational fluid dynamic. *International Journal of Advanced Robotic Systems*, 15(2). doi: <https://doi.org/10.1177/1729881418766190>
- Yadav, S., Gangwar, S., Singh, S. (2017). Micro/Nano Reinforced Filled Metal Alloy Composites: A Review Over Current Development in Aerospace and Automobile Applications. *Materials Today: Proceedings*, 4, pp. 5571-5582. doi: <https://doi.org/10.1016/j.matpr.2017.06.014>
- Yongchang, Y., Zhang, S., Li, H., Wang, X., Tang, Y. (2017). Modal and Harmonic Response Analysis of Key Components of Ditch Device Based on ANSYS, *Procedia Engineering*, 174, pp. 956–64, doi: <https://doi.org/10.1016/j.proeng.2017.01.247>
- См, Егер. (1986). Основы автоматизированного проектирования самолетов.Машиностроение, pp. 232, Москва. Retrieved from: <https://www.dissercat.com/content/avtomatizatsiya-dokumentirovaniya-protsesta-formirovaniya-otseka-magistralnogo-samoleta>